Engineering Structures 353 (2026) 122195

Contents lists available at ScienceDirect

Engineering Structures

journal homepage: www.elsevier.com/locate/engstruct

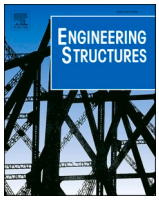

Innovative evaluation of precast, prestressed adjacent box beam bridges

Yugesh Maharjan, Suraj Dhungel, Serhan Guner *

Department of Civil and Environmental Engineering, University of Toledo, Toledo, OH 43606, USA

ARTICLE INFO

Keywords:
Maximum moment
Adjacent box beam bridges
Bridge evaluation
Custom vehicles
Load rating
Multicell
Permit loads

ABSTRACT

Load rating, the process of evaluating a bridge's safe live load capacity, is a critical aspect of bridge evaluation. Despite their prevalence, adjacent box beam bridges lack specialized methodologies and automated tools for their load rating. Engineers often resort to time-consuming, complex hand calculations or general-purpose tools that are not ideal for these unique bridges. This study addresses this challenge by developing a specialized computational methodology and an innovative computer tool for accurate, reliable, and rapid load rating of adjacent box beam bridges. The research accounts for diverse configurations, including skewed or non-skewed spans, composite and non-composite, and single or multicell beam sections; analyzes flexure and shear; assesses stresses at all critical locations for strength and service limit states; calculates capacities; and provides final load rating factors. A key innovation is its ability to identify the most critical location by precisely determining the exact maximum moment location, beyond conventional methods. It also evaluates shear at all potentially critical points, not just typical ones. The adopted shear flow approach enables the analysis of multicell box beam sections. To transfer these advancements to practice, the first specialized computer tool is developed for the load rating of adjacent box beam bridges. This tool is capable of rating 15 standard vehicles and custom vehicles with up to 35 axles. It also generates moment and shear envelopes for all vehicle types, assisting manual calculations or other analyses for various bridge types. Verification of the methodology and tool against 18 existing bridges using independent hand calculations and general-purpose software confirmed their high accuracy and reliability. A coefficient of determination of 0.974 or higher, a root mean square error (RMSE) of 0.251 or lower, a normalized RMSE of 7.43 % or lower and a bias close to zero are obtained.

1. Introduction

Precast prestressed adjacent box beam bridges are a bridge type constructed using precast concrete box beams placed side-by-side and linked together with shear keys, diaphragms, and post-tensioning. These bridges are simply supported, which may be skewed or non-skewed, with either composite or non-composite beams (Fig. 1). They are a common component of the United States' bridge inventory, accounting for 27 % of the bridge inventory in the State of Ohio [1]. Used primarily for short to medium spans, box beam bridges offer advantages due to their favorable span-to-depth ratio, rapid construction, and aesthetic appeal.

Bridge evaluation is the systematic process of assessing the structural condition, load-carrying capacity, and overall performance of an existing bridge to ensure its safety and serviceability under current and anticipated loading conditions [2]. Load rating is a critical part of bridge evaluation, in which an existing bridge is evaluated to determine its safe live load-carrying capacity based on the design and prevailing site conditions. It has significant implications for public safety (e.g., safe load limits), bridge management and prioritization (e.g., load posting, rehabilitation or replacement, and overweight vehicle permits), compliance with regulations (i.e., the National Bridge Inspection Standards [3] require all bridges in the national inventory to be load rated), and asset management (e.g., optimizing resource allocation and extending the lifespan of bridges). Despite the popularity of adjacent box beam bridges, the availability of computational methodologies and automated tools for their load rating lags behind those for other types of bridges. The use of general-purpose load rating tools for adjacent box beam bridges requires expert-level customizations, is time-consuming, and has limitations due to incomplete vehicle types and the need for multiple analyses to account for numerous design configurations across the wide range of box beam sections used over the years. In addition, the general-purpose load rating tools produce an excessive amount of output that requires expert knowledge and significant post-processing effort to

* Corresponding author.
E-mail addresses: yugesh.maharjan@rockets.utoledo.edu (Y. Maharjan), suraj.dhungel@rockets.utoledo.edu (S. Dhungel), serhan.guner@utoledo.edu (S. Guner).

https://doi.org/10.1016/j.engstruct.2026.122195
Received 4 July 2025; Received in revised form 21 December 2025; Accepted 18 January 2026
Available online 22 January 2026

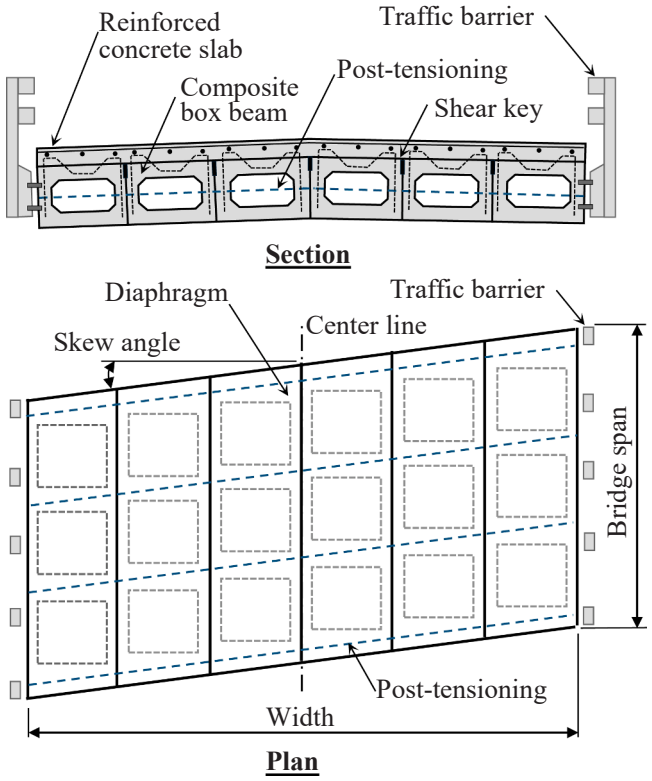

Fig. 1. Typical plan and section of skewed adjacent box beam bridge with composite beams.

understand.

To address the aforementioned gaps, this study has developed a specialized computational methodology and an innovative computer tool, named AD-BOX, for accurate, reliable, and rapid load rating of adjacent box beam bridges. The research aims to account for skewed or non-skewed spans with composite and non-composite cross sections; analyze for flexure and shear; consider both single and multicell box beam sections; assess stresses at all potentially critical locations for strength and service limit states; calculate capacities; and provide final load rating factors.

An important aspect of the methodology is its capability to determine the critical location with the maximum load effect and the minimum rating factor. The methodology calculates the maximum moment capacity at the exact location of the maximum moment instead of the conventional one-tenth-of-the-span method. This approach improves accuracy while reducing the analysis output and minimizing the engineering effort. The shear load rating is evaluated not only at typical shear critical locations but also at other potentially critical locations. It is also capable of evaluating the box beam sections with multicell configurations, which is achieved by a more accurate analysis of the torsional behavior based on a shear flow approach.

To facilitate the proper application of the methodology, an innovative computer tool, which is the first computer tool specialized in the load rating of adjacent box beam bridges, is developed using the Visual Basic for Applications (VBA) programming language. Developed with approximately 3000 lines of code, the algorithm is incorporated into an MS Excel Spreadsheet to create the computer tool AD-BOX. This approach is intended to provide engineers and researchers with a familiar working environment without the need to install and learn a new computer program. The tool is capable of load rating 15 standard vehicle types and extra-long custom vehicles with up to 35 axles. A high axle count is selected to account for vehicles that may emerge in the future. A wide range of vehicle configurations is included to cover all possible scenarios. The 15 vehicle types include the design vehicle, legal

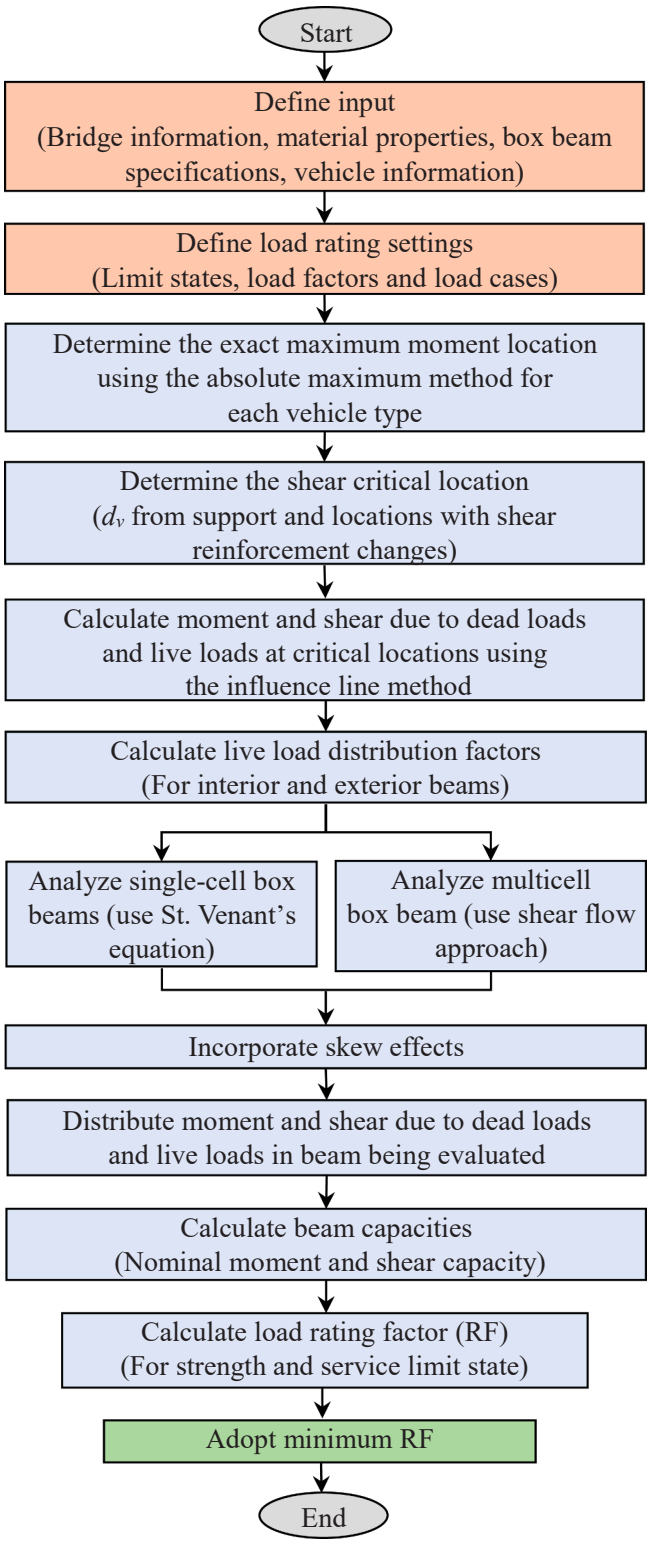

Fig. 2. Flow chart of the methodology.

loads, special hauling vehicles, and permit loads. The tool also provides the capability to generate moment and shear envelopes for the selected vehicle type on the bridge, for use in manual calculations or other analyses. The accuracy and reliability of the methodology and computer tool are assessed and verified by load rating 18 bridges for 15 vehicle types and four custom vehicles, using independent hand calculations and a general-purpose load rating software.

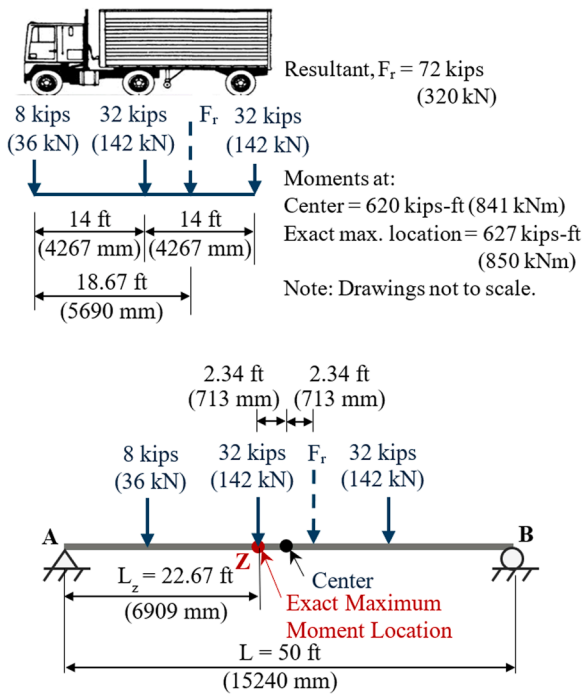

Fig. 3. Exact maximum moment location due to a vehicle type, HL-93 on a 50 ft (15240 mm) simply supported bridge.

2. Methodology

The main steps of the developed methodology are presented in Fig. 2. The proposed methodology requires essential input, including bridge geometry, material properties, box beam specifications, and vehicle information. Load rating settings, such as limit states, load factors, and load cases, are established to ensure compliance with the relevant design standards [2,4].

The dead loads (DC and DW) and live loads are considered in the load rating. DC includes self-weight of the structural components, while DW covers the weight of wearing surfaces and utilities. Live loads include a range of vehicle loading scenarios, including design, legal, and permit vehicles. The HL-93 design vehicle, adopted in the United States and selected as a representative design vehicle worldwide. Legal loads are the maximum allowable vehicle weights permitted on public highways without special hauling permits, typically including 2- and 3-axle trucks and 4- to 7-axle semi-trailer combinations. This study includes three Ohio legal loads (2F1, 3F1, 5C1 with 2-, 3-, and 5-axles) and three AASHTO legal loads (Type 3, Type 3S2, Type 3–3 with 3-, 5-, and 6-axles). To represent closely spaced multi-axle single-unit trucks introduced in the last decade, such as dump trucks, construction vehicles, and solid waste trucks, which produce higher effects than legal models, four special hauling vehicles (SU4, SU5, SU6, and SU7 with 4-, 5-, 6- and 7-axles) and two emergency vehicles (EV2 and EV3 with 2- and 3- axles) are included. In addition, two permit loads (PL 60 T and PL 65 T with 6- and 7-axles), which exceed the legal weight and dimensional limits and require special approval are also included. The detailed configurations of the selected vehicles for this study are presented in Appendix A.

Based on the vehicle type, the load rating is performed under the inventory and operating conditions. The load factors are selected accordingly, based on the vehicle type and the applicable limit states. In the inventory conditions, both the strength and service limit states are evaluated, whereas in the operating conditions, only the strength limit state is required, with the service limit state considered optional. The design vehicles are assessed under both inventory and operating conditions, while all other vehicles are evaluated under the operating conditions.

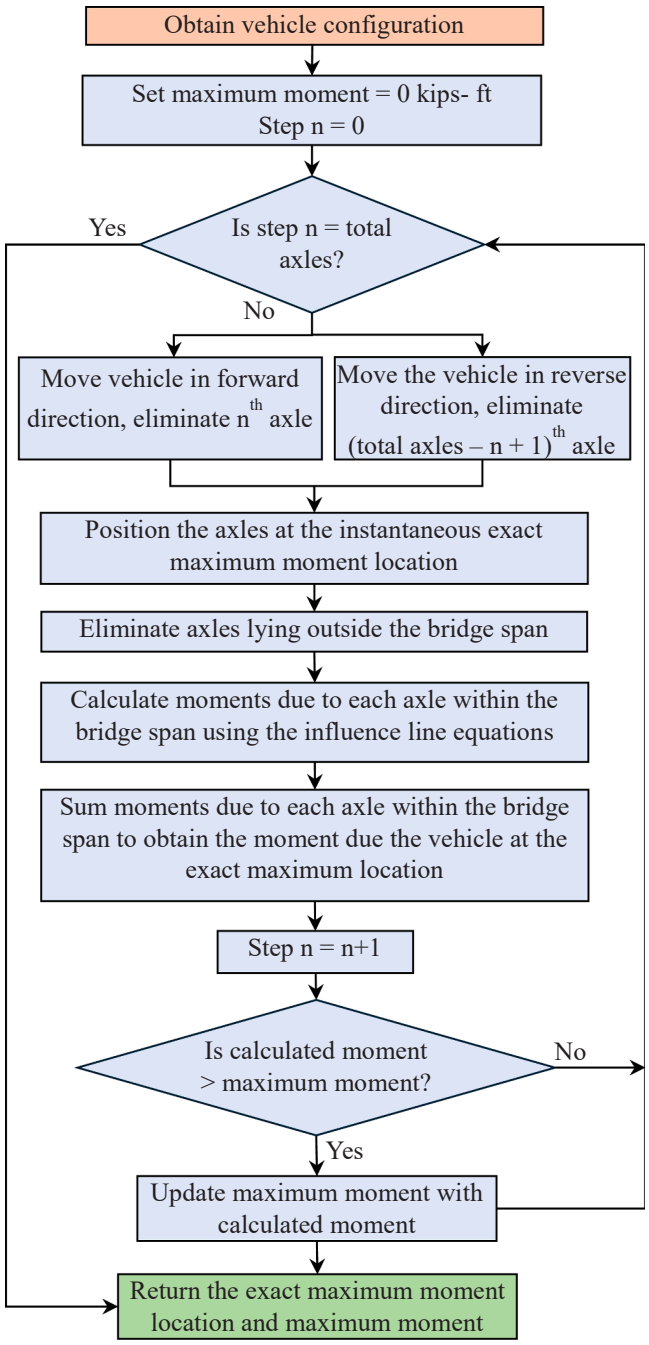

Fig. 4. Flow chart of the absolute maximum method.

2.1. Exact maximum moment location

The conventional one-tenth-of-the-span method estimates the maximum moment by positioning the vehicle loads at regular intervals along the span, typically from the support to midspan. The highest calculated moment is then selected as the maximum moment. However, the preset one-tenth intervals are unlikely to capture the exact maximum moment and thus may be less accurate. In addition, a large amount of output is created for locations that will not govern.

A more refined approach, the absolute maximum method used in this study, involves the determination of the exact location of the maximum moment. This approach improves accuracy and reduces the amount of calculations and output. With the concept that critical moments generally arise under the largest axle load positioned closest to the system's resultant force, this method simplifies the determination of the

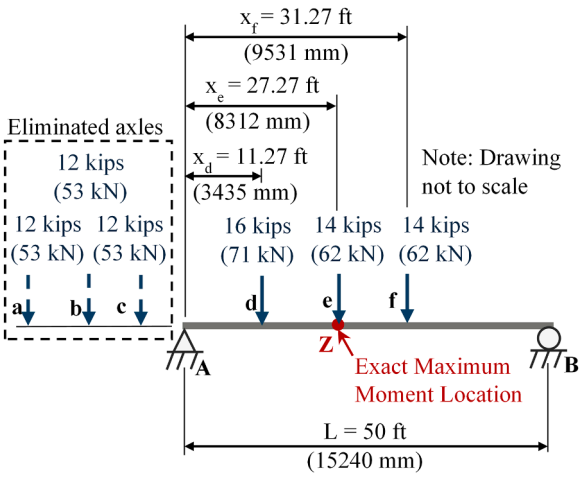

Exact max. location = 27.27 ft (8312mm) from the support
Moment at:
Center = 394 kips-ft (534 kN-m)
Exact max. location = 399 kips-ft (541 kN-m)

Fig. 5. Exact maximum moment location due to a vehicle type, Type 3–3 with some axles lying outside a 50 ft (15240 mm) simply supported bridge.

maximum moment. The absolute maximum method can be stated as the exact maximum moment location, for any vehicle type on a simply supported bridge, occurs where the axle closest to the resultant of all axles within the span is positioned equidistant from the resultant and the center of the bridge. The maximum moments due to the live loads and dead loads are evaluated at this exact location. An example involving a vehicle type, HL-93, is shown in Fig. 3.

The determination of the exact maximum moment location becomes challenging for longer vehicles with an axle or some axles lying outside the bridge span. Only the axles lying within the bridge span should be considered for the calculation. The challenging aspect is to determine which axles shall be eliminated, which requires an iterative calculation process. An algorithm is developed for this purpose, which replicates each vehicle type moving in both forward and reverse directions. At each vehicle position, the moment produced by each axle lying within the bridge span is calculated using the influence line equations, as explained in 2.3. The algorithm then evaluates whether the sum of moments due to each axle yields the instantaneous maximum moment, or if eliminating one or more end axles results in a higher value. In each iteration, the algorithm eliminates the end axles one at a time, repeating the process to determine the axle combination that produces the maximum moment among all possible combinations. The exact maximum moment location with the corresponding maximum moment for each vehicle type on the bridge is then captured as the output. The flowchart illustrating the algorithm developed is presented in Fig. 4.

An example of the exact maximum moment location due to a long vehicle with some axles lying outside the bridge span, Type 3–3 is shown in Fig. 5.

2.2. Shear critical locations

The typical shear critical point on a simply supported bridge is located at a distance equal to the effective shear depth d_v away from the face of bearings at the supports according to major design codes (e.g., AASHTO LRFD 2024 [4], CSA S6–19 2019 [5], PCI 2024 [6]).

In addition to evaluating shear at the typical shear critical section, it is important to assess shear at other locations along the bridge, particularly where the shear reinforcement or its spacing changes. Inspection of the design drawings of several adjacent box beam bridges located in the State of Ohio reveals that the provided shear reinforcement varies

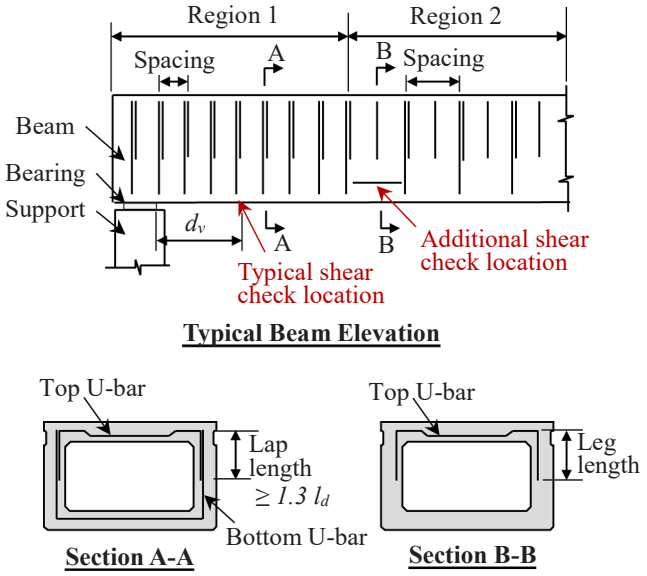

Fig. 6. Typical beam elevation and sections showing typical and additional shear check locations.

Table 1
Nominal shear capacity and shear rating factors across the bridge span.

	Distance from the left support, ft (mm)	Nominal shear capacity, kips (kN)	Rating factors (RFs)	
Region 1	1 (304.8)	200.74 (893)	2.426	
	1.8 (548.6)	200.74 (893)	2.492	Typical shear check location
	2 (609.6)	200.74 (893)	2.512	
	3 (914.4)	200.74 (893)	2.603	
	4 (1219.2)	200.74 (893)	2.700	
Region 2	5 (1524)	138.46 (616)	1.819	Shear critical location
	6 (1828.8)	138.46 (616)	1.896	
	7 (2133.6)	138.46 (616)	1.978	
	8 (2438.4)	138.46 (616)	2.067	
	16 (4876.8)	138.46 (616)	3.080	
	31 (9448.8)	138.46 (616)	5.869	Midspan

along the bridge span. Consider, for example, the bridge span shown in Fig. 6. In Region 1, a complete set of U bars, both top and bottom, is provided, with a lap length not less than 1.3 times the development length (l_d), as shown in Section A-A. Region 2 contains a complete set of U bars and only the top U bar at alternate locations, as depicted in Section B-B. Due to insufficient development length, the alternately placed top U bar in Region 2 does not act as shear reinforcement, resulting in a reduced nominal shear capacity due to the increased stirrup spacing. Consequently, the shear load rating becomes critical at Region 2 rather than at the typical shear critical section (Table 1). To capture such a possibility, the developed methodology and computer tool perform additional shear checks at locations where shear reinforcement or spacing changes.

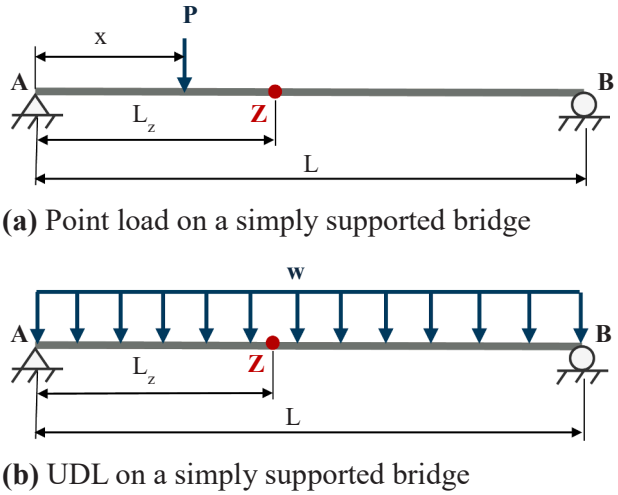

Fig. 7. Schematic diagrams defining variables used in the equations.

2.3. Maximum moment and shear

For load rating in flexure, the maximum moment due to the dead and vehicle loads is calculated at the exact maximum moment location determined using the absolute maximum method. The maximum moment is calculated using the influence line equations given by Eq. (1) to Eq. (3), based on the type of load, either point load P or uniformly distributed load w on the bridge span L as shown in Fig. 7. For each vehicle type, the moments M_z due to each axle within the bridge span are calculated as point loads at the exact maximum moment location Z, located at the distance L_z from the support and are summed to obtain the maximum moment due to the vehicle type.

$$M_z = P \times \left[\left(1 - \frac{x}{L}\right) \times L_z - (L_z - x)\right]; \text{ for } 0 < x \le L_z \tag{1}$$

$$M_z = P \times \left[\left(1 - \frac{x}{L}\right) \times L_z\right]; \text{ for } L_z \le x < L \tag{2}$$

$$M_z = \frac{w \times L_z}{2} \times (L - L_z); \quad \text{for} \quad 0 \le L_z \le L \tag{3}$$

For load rating in shear, the shear critical location is either at the typical shear check location or locations where the shear reinforcement or its spacing changes. The shear force due to the dead and vehicle loads is calculated at these locations using the influence line equations given by Eq. (4) to Eq. (6), based on the type of the load as shown in Fig. 7. For the vehicle loads, the maximum shear is obtained when the axle with maximum load among the end axles after eliminating those lying outside the bridge span is placed at the location being considered for the evaluation. The shear force V_z due to each axle within the bridge span is calculated as a point load at these locations and summed to obtain the maximum shear due to the vehicle.

$$V_z = P \times \left(-\frac{x}{L}\right); \text{ for } 0 < x < L \tag{4}$$

$$V_z = P \times \left(1 - \frac{x}{L}\right); \text{ for } L_z \le x < L \tag{5}$$

$$V_z = w \times \left(\frac{L}{2} - L_z\right); \text{ for } 0 \le L_z \le L \tag{6}$$

2.4. Load distribution factors

The moment and shear due to the dead and vehicle loads must be appropriately distributed among all beams within the bridge system. The self-weight of the beam and any permanent loads, such as barriers and wearing surfaces, are uniformly distributed across the beams since adjacent box beam bridges meet the required conditions.

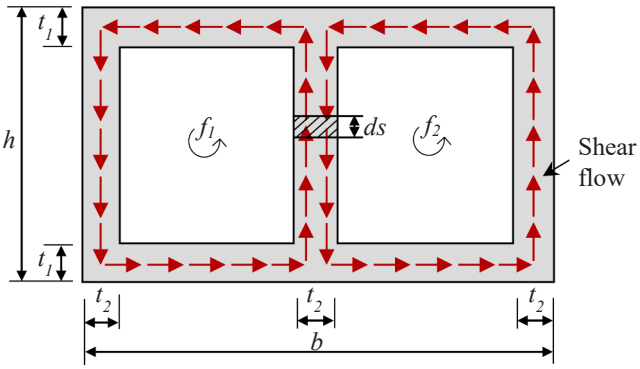

Fig. 8. Typical multicell box beam section with two cells.

The live load distribution factors are determined to account for the proportional effects of the live loads for each beam. Several methods, including the lever rule, uniform distribution method, and finite element method may be implemented to determine the live load distribution factors [7,8]. For the box beam bridges, simplified methods involving the use of empirical equations, calibrated from the aforementioned methods, are found to be reasonably accurate for determining the live load distribution factors [9,10]. This simplified method has been adopted in commonly used standards such as AASHTO LRFD (2024) [4] as the distribution factor method and is therefore also adopted in this methodology. For both interior and exterior beams, distinct empirical equations for the live load distribution factors for cases of one design lane loaded, and two or more design lanes loaded are used. The maximum value is adopted as the governing distribution factor. The simplified equations used in this method are presented in Appendix B.

Determining the live load distribution factors for adjacent box beams using the distribution factor method requires computation of the torsional constant, which is dictated by the beam's geometry. The torsional constant for beams with single-cell geometry can be easily calculated using the St. Venant equation; however, those with multi-cell configurations require a different approach as described below.

2.5. Single-cell box beams

The St. Venant torsion theory is applicable to closed, thin-walled sections, such as single-cell box beams, where torsional deformation is primarily resisted by the uniform shear flow around the perimeter of the cross-section, through their closed geometry and symmetric distribution of material [4,11]. In such sections, the cross-sectional warping is minimal and can typically be neglected, allowing the torsional response to be accurately characterized. The St. Venant equation for determining the torsional constant is expressed in Eq. (7).

$$J = \frac{4 A_o^2}{\sum \frac{s}{t}} \tag{7}$$

where J is the torsional constant; A_o is the area enclosed by the centerline of elements of the beam; and s is the length of the side element.

2.6. Multicell box beams

Multicell box beams introduce additional complexity due to the presence of multiple cells formed by the middle webs. The torsional constant for such sections cannot be directly calculated using the St. Venant equation. The proposed methodology uses a shear flow approach to derive the required torsional constant. Fig. 8 illustrates the distribution of the shear flow in the multicell box beams with two cells where the

shear flow direction is represented by the red lines. Each cell in the box beam exhibits a distinct shear flow, represented as f_1 and f_2 for cells 1 and 2, respectively. The shear flow in the adjacent cell affects the calculation of the twist in each cell. In the shared webs between cells 1 and 2, the shear flows act in opposite directions.

In the figure, b is the width of the beam section; h is the height of the beam section; t_1 is the thickness of the beam flange section; and t_2 is the thickness of the beam web section.

The total torque (T) carried by the cross-section with an n-number of cells is expressed by Eq. (8).

$$T = \sum_{i=1}^{n} 2 f_i A_{mi} \tag{8}$$

where A_{mi} is the centerline area of i^{th} cell, and f_i is the shear flow in i^{th} cell. Twist per unit (θ) length in each cell can then be found by Eq. (9).

$$\theta = \frac{1}{2GA_{mi}} \int_0^{l_{mi}} \frac{f_i - f_j}{t} ds, \quad i = 1, 2, \ldots, n \tag{9}$$

where l_{mi} is the length of the mean perimeter of the i^{th} cell, G is the shear modulus, f_j is the shear flow of the cell adjacent to the i^{th} cell where ds is located, t is the thickness where ds is located.

In a multicell box beam, the shear flow within each cell remains constant, and the angles of twist are uniform across all cells. Therefore, the unknown shear flow in each cell ($f_1, f_2, f_3, \ldots,$ and f_i) can be determined by equating the twists of each cell from Eq. (9). After determining the shear flow for each cell, the total torque (T) and twist (θ) can be determined from Eqs. (8) and (9) respectively. With T and θ determined, the torsional constant (J) is found using Eq. (10).

$$J = \frac{T}{G\theta} \tag{10}$$

More simplifications can be made if all cells have equal area or identical, when the opposite shear flows in adjacent cells cancel out, resulting in no effect on the torsion. In such condition, the equation for the torsional constant is reduced to the St. Venant's equation, and the area enclosed by the centerline of elements of the beam (A_o) and the length of the side element (s) should be calculated taking the beam as single-cell without the webs between the cells.

2.7. Skew effect

Skew occurs when the bridge span is not orthogonal to the bridge supports, typically due to spatial constraints or obstacles, either anthropogenic or natural. In the skewed bridges, the load path shifts toward the corners of the span at an angle greater than 90°, unlike non-skewed bridges, where the load path follows the direction of the span [12]. This alters the load distribution factors resulting in increased shear forces at the exterior girders with higher reactions at the corners with angles greater than 90° [13,14], and decreased longitudinal moments compensated by the development of transverse moments when compared to the non-skewed bridges [15]. To effectively distribute the moment and shear due to the live loads in each beam of the skewed bridge, correction factors are applied to the live load distribution factors calculated using the distribution factor method. The correction factors used to incorporate the skew effect are presented in Appendix B.

2.8. Nominal moment capacity

The nominal moment capacity can be determined using various methods, including the strain compatibility method and the rectangular stress block method. The strain compatibility method is a complex method requiring a detailed analysis of internal strains and corresponding stresses based on the actual stress-strain behavior of the materials, which is essential when the geometry of the section is non-rectangular or irregular, has non-concentric tendon profiles, non-symmetric reinforcement, and non-linear stress-strain across the section. In contrast, the rectangular stress block method is an approximate approach, where the compression zone in concrete is idealized as a uniformly distributed stress block, simplifying the analysis of internal forces. The adjacent box beams have rectangular sections with straight tendons installed symmetrically, with linear stress-strain behavior at the service loads. To determine the most suitable method for the developed methodology, a study was conducted on 18 sample bridges with the adjacent box beams, including both non-composite and composite sections. The nominal moment capacity calculated using the rectangular stress block method is found to be very close to that calculated using the strain compatibility method for both non-composite and composite beams based on a comparison for the 18 sample bridges. The mean of the ratios of the capacities using the rectangular stress block method divided by the strain compatibility method is found very close to 1.0 with a coefficient of variation (CV) up to 2.50 % as presented in Fig. 9. Thus, for the adjacent box beams, the moment capacity calculated using the rectangular stress block method is considered the suitable method for load rating purpose and is adopted in this study [16]. All relevant equations used for calculating nominal moment capacity are presented in Appendix C.

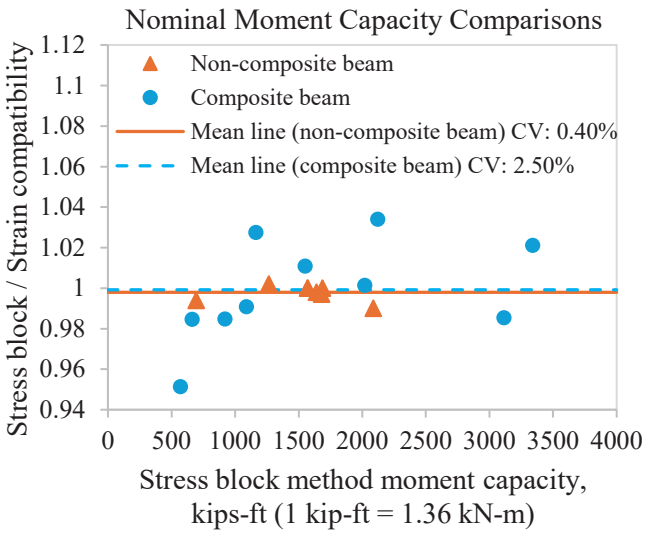

Fig. 9. Nominal moment capacity comparisons of the rectangular stress block method with the strain compatibility method for 18 sample bridges.

2.9. Nominal shear capacity

Shear capacity calculations exhibit considerable discrepancies across codes [4–6,17] with some relying on empirical curve fitting from the experimental data, while others adopt a more theoretically grounded approach. The proposed methodology integrates the Modified Compression Field Theory (MCFT) [18] for the shear capacity calculations. This theory offers a more refined approach to shear strength subjected to combined axial, shear and flexural stresses, accounting for key factors such as the diagonal cracking behavior of concrete under shear and interaction between longitudinal and transverse reinforcement under inelastic conditions.

To accurately determine the shear capacity using the MCFT, it is necessary to calculate both the shear strength factors (β), which reflect the ability of diagonally cracked concrete to transmit tension and shear, and the angle of inclination of the diagonal compressive stresses (θ). The values of β and θ depend on the net longitudinal strain in the section (ϵ_s), which is obtained through an iterative process based on the maximum shear demand (V_u) applied to the beam, considering the concurrent ultimate moment (M_u). It is also important to confirm that the longitudinal reinforcement has sufficient tensile capacity to resist the tension induced

LOAD RATING RESULTS

Compute Load Rating

Design Vehicles		
Loading Type	Rating Factor	
	Inventory	Operating
HL93	1.004	1.325

Ohio Legal Vehicles		
Loading Type	GVW	Rating Factor
	Tons	
2F1	15	3.234
3F1	23	2.165
5C1	40	2.206

Specialized Hauling Vehicles		
SU4	27	1.902
SU5	31	1.728
SU6	34.5	1.550
SU7	38.75	1.422

Emergency Vehicles		
EV2	28.75	2.085
EV3	43	1.613

AASHTO Legal Vehicles		
Type3	25	2.146
Type3S2	36	2.018
Type3_3	40	2.170

Permit Vehicles		
PL60T	60	2.071
PL65T	65	1.602

Custom Vehicle		
Custom Vehicle 1	65	2.085

Fig. 10. AD-BOX interface showing the output section.

by shear. This requirement is verified using the longitudinal reinforcement criterion based on the equilibrium, which ensures that the longitudinal tension reinforcement in flexure is adequate to achieve the calculated shear capacity. If the equilibrium is not satisfied, an iterative procedure can be performed in which the shear capacity is reduced based on the maximum shear demand, along with the concurrent moment that can be applied to the beam, until the longitudinal reinforcement criterion is satisfied [19]. All relevant equations for these calculations are provided in Appendix C.

2.10. Load rating factor

The proposed methodology employs the load and resistance factor rating (LRFR) method for the strength limit states and the allowable stress design (ASD) method for the service limit states [2]. The serviceability checks include time-dependent prestress losses such as elastic shortening, creep, shrinkage, and relaxation [4,6,20].

Based on the vehicle types, the load rating is comprised of three distinct procedures: design, legal, and permit load ratings. The rating factors for each vehicle type are determined using the general expression given by Eq. (11).

$$RF = \frac{C - (\gamma_{DC})(DC) - (\gamma_{DW})(DW) \pm (\gamma_P)(P)}{(\gamma_{LL})(LL + IM)} \tag{11}$$

where RF is the rating factor for the live load carrying capacity; C is the capacity of the structural member, with appropriate adjustments made for the structural conditions; γ_{DC} and γ_{DW} are the factors for the dead loads DC and DW respectively; γ_{LL} is the factor for live loads; IM is the impact factor; γ_P is the factor for the permanent loads P other than the dead loads. These factors are selected according to the relevant standards of the load rating authority. More information can be found on the reference [2,16].

The final load rating is performed at the moment critical and shear critical locations, with the lowest value controlling the load rating factor.

2.11. Computer tool AD-BOX

To execute the proposed specialized methodology and perform the load rating calculations, an innovative computer tool, AD-BOX: Adjacent Box Beam Bridges Analysis and Rating [21], is developed using the Visual Basic for Applications (VBA) programming language and implemented into a Microsoft Excel spreadsheet. This approach is intended to provide engineers and researchers with a familiar working environment without the need to install or learn a new computer program. The tool is shared as freeware for the use of the engineering community.

As the first computer tool specialized in the load rating of adjacent box beam bridges, the tool employs a user-friendly interface for input and output. The input is logically organized into labeled sections requiring bridge geometry, material properties, design parameters, and load rating settings. To minimize user input errors, dropdown menus linked to the standard reference tables, including a complete list of the standard box beam sections [22] as well as options for addition of custom sections, are included in the tool. Developed with approximately 3000 lines of VBA code, the tool executes the formulations of the proposed methodology, automatically calculating the loads, distribution factors, bending moments, shear forces, and beam capacities based on the user-provided input, and ultimately generating the rating factors as output.

The tool can evaluate bridges for the 15 vehicle types presented in Appendix A. These include the standard vehicles required for the load rating in the United States, including the state of Ohio [23]. The output rating factor (RF) results are organized based on the vehicle type, as shown in Fig. 10. To address the future needs, the tool also accommodates extra-long custom vehicles with up to 35 axles.

Built-in error and warning messages are incorporated to help engineers and researchers identify and resolve potential input issues early in the process, thereby enhancing the reliability of the results. The tool checks the load rating results for unusual values and prompts the user in the case of potential input errors. In addition, detailed calculations involved in each computation step are provided. Access to all detailed calculations involved in the evaluation facilitates a deeper understanding, thereby intuitively educating the engineers and researchers in the proper application of the methodology.

To allow engineers to use the developed tool for any type of simply supported bridge, an algorithm is developed, which can generate moment and shear envelopes for each of the 15 standard vehicle types and extra-long custom vehicles. The algorithm presents these envelopes in both tabular and chart formats. The tabular format enables engineers to copy the values for use in other analysis software or for independent hand calculations, while the chart format offers a visual representation of the envelopes, highlighting their variation along the span and identifying the peak values.

3. Verification of the methodology

Eighteen sample bridges were load rated using the developed computer tool, independent hand calculations, and general-purpose load rating software. These sample bridge drawings are provided by the Ohio Department of Transportation (ODOT) for research purposes. The samples include a total of seven non-skewed bridges (all with single-cell box beam configurations, three non-composite and four composite cross-

Table 2
Summary of the sample bridges used in the verification.

Bridge sample	Year of construc-tion	Design span ft (mm)	Beam type	Skew/ Non-skew	Skew (Degrees)
Single-cell box beam bridges					
1	2024	30 (9144)	Non-composite	Non-skew	0
2	2018	50 (15240)	Non-composite	Non-skew	0
3	1982	62 (18898)	Non-composite	Non-skew	0
4	2023	25 (7620)	Composite	Non-skew	0
5	2021	45 (13716)	Composite	Non-skew	0
6	2018	55 (16764)	Composite	Non-skew	0
7	2021	80 (24384)	Composite	Non-skew	0
8	2018	42 (12802)	Non-composite	Skew	28
9	1984	65 (19812)	Non-composite	Skew	5
10	2009	65.5 (19964)	Non-composite	Skew	12
11	1985	74.85 (22814)	Non-composite	Skew	30
12	2016	75 (22860)	Non-composite	Skew	10
13	2021	26 (7924)	Composite	Skew	30
14	2022	47.71 (14542)	Composite	Skew	19
15	2018	60 (18288)	Composite	Skew	24
16	2019	83 (25298)	Composite	Skew	20
Multicell box beam bridges					
17	1996	35 (10668)	Composite	Skew	30
18	2007	45 (13716)	Composite	Skew	10

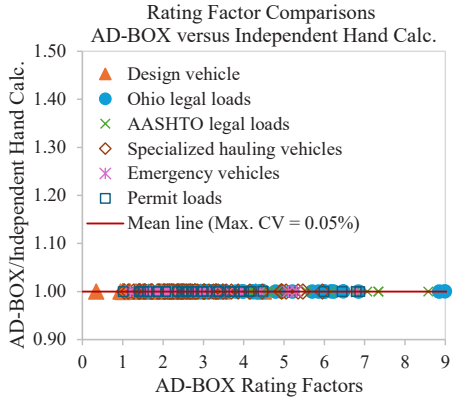

Fig. 11. Rating factor comparison of proposed methodology to independent hand calculations of 18 sample bridges for 15 vehicle types.

sections) and eleven skewed bridges (nine with single-cell and two with multicell beam configurations, five with non-composite and six with composite cross-sections). Such a diverse selection of bridge types was made on purpose for a more in-depth examination of RF values for all 15 vehicle types and four extra-long custom vehicles. The analyzed vehicle configurations cover axle counts from 2 to 35, with various spacings, and gross vehicle weights ranging from 30 kips (133 kN) to 670 kips (2980 kN). The summary of the sample bridges used in the verification is presented in Table 2; the complete details may be found in reference [16].

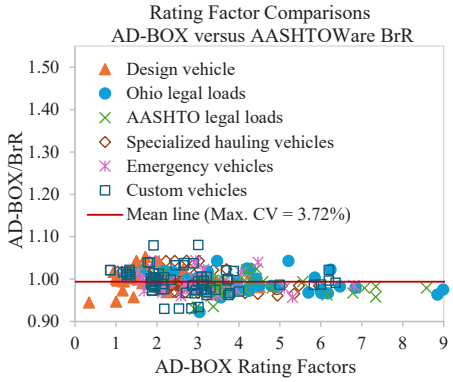

Fig. 12. Rating factor comparison of proposed methodology to general-purpose load rating tool of 18 sample bridges for 15 vehicle types and four custom vehicles.

3.1. Independent hand calculations

The hand calculations involved detailed calculations of moments and shear due to the dead and live loads, determination of the critical locations, calculation of the live load distribution factors including skew effects, followed by calculations of beam capacities and final load rating factors. For a single bridge and a single vehicle type, the hand calculations typically require approximately 50 pages (refer to Appendix B of reference [16]). Extending this process to all vehicle types would result in several hundred pages for a single bridge alone. As such, the hand calculations are infeasible, considering approximately 8000 adjacent box beam bridges in the state of Ohio alone [1].

The verification for all 15 vehicle types consistently resulted in a mean of nearly 1.0, represented by the mean line in Fig. 11, with a coefficient of variation (CV) close to 0 %, for the rating factor (RF) ratios of the proposed methodology divided by independent hand calculations, confirming the accuracy of the proposed methodology. Detailed verification results are provided in reference [16].

3.2. General-purpose load rating software

The load rating results from AD-BOX are compared with those from the BR100 summary sheets provided by ODOT, containing results from the load rating software, AASHTOWare BrR [24]. The RF values for all 18 bridges were compared for 15 vehicle types and four custom vehicles (four custom vehicles with 12, 15, 19, and 35 axles). The 35-axle extra-long vehicle is a hypothetical vehicle created to assess the performance and reliability of the methodology for such vehicle types. The verification for all 15 vehicle types and four custom vehicles consistently resulted in a mean of approximately 1.0, represented by the mean line in Fig. 12, with a CV up to 3.72 %, for the RF ratios of the proposed methodology divided by BrR, confirming the reliability of the proposed methodology. Detailed verification results are provided in reference [16].

3.3. Statistical Evaluation

The evaluation was performed using four statistical metrics: coefficient of determination (R^2), Root Mean Square Error (RMSE), normalized RMSE (nRMSE), and bias. The R^2 value measures the degree of correlation between the results computed by each method and the independent hand calculation as reference results, with values close to 1.0 indicating a strong agreement. RMSE quantifies the average magnitude of the deviations between the computed and reference results, where smaller values indicate higher accuracy. The normalized RMSE

Table 3
Statistical metrics for rating factor comparisons of AD-BOX, BrR and independent hand calculations.

Statistical Metrics	AD-BOX versus Hand Calc.	BrR vs. Hand Calc.	AD-BOX versus BrR
R^2	1.000	0.974	0.974
RMSE	0.000	0.251	0.223
nRMSE	0.02 %	8.14 %	7.43 %
Bias	0.000	0.016	-0.017

expresses RMSE relative to the mean of the reference results, allowing the comparison across different scales; values below 10 % indicate a strong agreement. Bias represents the mean signed difference between the computed and reference results, where values close to zero indicate minimal systematic overestimation or underestimation.

Table 3 presents the calculated statistical metrics while Fig. 13 presents the correlation plots. The results demonstrate an excellent agreement among the three methods with R^2 of 0.974 or lower. The low RMSE and nRMSE of less than 10 % further confirm the accuracy and reliability of the proposed methodology and the developed computer tool. The low values of bias (close to zero) indicate minimal difference in calculated results.

4. Summary and conclusions

This study proposes a specialized computational methodology and an innovative computer tool, AD-BOX (Adjacent Box Beam Bridges Analysis and Rating), developed to improve the accuracy and reliability of load rating for simply supported adjacent box beam bridges. The methodology explicitly addresses complexities arising due to the presence of composite cross-sections, skew effects, and both single-cell and multicell box beam configurations.

The proposed methodology provides reliable and accurate load ratings applicable to all design, legal, and permit load ratings for a wide range of vehicles. It accommodates load ratings for 15 standard vehicle types and extra-long custom vehicles with up to 35 axles, ensuring a versatile solution for the needs that may arise in the future. Verification of the methodology involved load ratings of 18 sample bridges for the 15 vehicle types and four custom vehicles, utilizing the developed tool, independent hand calculations, and general-purpose load rating software. The results of the studies conducted support the following conclusions:

1. The proposed methodology and the developed computer tool provides accurate and reliable load rating process for adjacent box beam bridges, while significantly reducing the engineering effort and potential input errors through automated computations and checks.
2. The proposed methodology improves accuracy by precisely determining the maximum moment due to the vehicle loads at the exact maximum moment location, instead of the conventional one-tenth-of-the-span method.
3. Shear load rating is performed through a comprehensive shear analysis at all potentially shear critical locations, including the typical shear check location and other points where the shear reinforcement or its spacing changes, ensuring the correct identification of the critical rating factors in shear.
4. A more accurate analysis of the torsional behavior is achieved based on the beam's specific geometry by utilizing St. Venant's equation for single-cell and shear flow approach for multicell box beams.
5. The proposed methodology and developed computer tool accurately load rate standard and extra-long vehicles, delivering reliable results for all configurations considered. Verification results confirm this accuracy, with rating factor (RF) ratios (proposed methodology vs. hand calculations) showing a mean of approximately 1.0 and a coefficient of variation (CV) of nearly 0 %.
6. Comparison results confirm the reliability of the methodology and developed computer tool. The RF ratios from the computer tool, when divided by those from general-purpose load rating software, show a mean of approximately 1.0 with a coefficient of variation (CV) up to 3.72 %.
7. The statistical metrics, including a coefficient of determination of 0.974 or higher, a root mean square error (RMSE) of 0.251 or lower, a normalized RMSE of 7.43 % or lower and a bias close to zero further confirm the accuracy and reliability of the proposed methodology and the developed tool.
8. By transferring the research findings to engineers and researchers, the developed computer tool enables accurate load rating of adjacent box beam bridges while intuitively educating users and addressing real-world load rating challenges.

CRediT authorship contribution statement

Yugesh Maharjan: Writing – original draft, Software, Methodology, Investigation, Formal analysis, Data curation. **Suraj Dhungel:** Writing – original draft, Visualization, Validation, Investigation. **Serhan Guner:** Writing – review & editing, Supervision, Resources, Project administration, Funding acquisition, Formal analysis.

Funding source

This work is supported by the Ohio Department of Transportation [PID: 120635].

Declaration of Competing Interest

The authors declare the following financial interests/personal relationships which may be considered as potential competing interests: Yugesh maharjan, Suraj Dhungel and Serhan Guner report financial support was provided by Ohio Department of Transportation. They

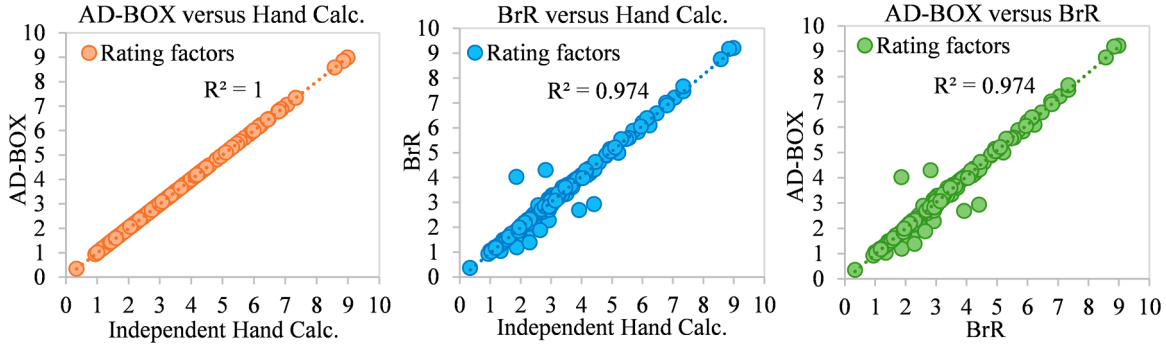

Fig. 13. Correlation plots for rating factor comparisons of AD-BOX, BrR and independent hand calculations.

declare that they have no known competing financial interests or personal relationships that could have appeared to influence the work reported in this paper.

Acknowledgments

The authors would like to thank the Ohio Department of Transportation (ODOT) for funding and supporting this research. The research team is grateful to the Technical Advisory Committee members: Mr. Amjad Waheed, PE, Administrator, and Mr. Grant Austin, Transportation Engineer, for providing verification materials and continuous feedback and support. We also acknowledge Ms. Vicky Fout, ODOT Statewide Planning and Research, for managing the project. The authors are also grateful to the Department of Civil and Environmental Engineering at the University of Toledo, Ohio, United States, for providing the facilities needed for this research.

Appendix A. Supporting information

Supplementary data associated with this article can be found in the online version at doi:10.1016/j.engstruct.2026.122195.

Data Availability

The authors do not have permission to share data.

References

[1] Abu-Hajar O. Ohio pilot projects using corrosion resistant prestressing strands. ASPIRE Spring 2023;2023:34–7. ⟨https://lsc-pagepro.mydigitalpublication.com/publication/?i=786437&p=36&view=issueViewer&pp=1⟩.
[2] AASHTO MBE. AASHTO Manual for Bridge Evaluation. 3rd Edition. Washington, DC, U.S.A.: American Association of State Highway and Transportation Officials; 2018–22. p. 749 (Customary US units).
[3] FHWA (2022) "National Bridge Inspection Standards," Federal Highway Administration. FHWA Docket No. FHWA–2017–0047, Washington, DC, U.S.A. <⟨https://www.fhwa.dot.gov/bridge/nbis.cfm⟩>
[4] AASHTO LRFD. AASHTO LRFD Bridge Design Specifications. 10th Edition. Washington, DC, U.S.A.: American Association of State Highway and Transportation Officials; 2024. p. 1905 (Customary US units).
[5] Canadian Standards Association. Canadian highway bridge design code (CSA S6-19). 9th Edition. Canada: Canadian Standards Association, Toronto, Ontario; 2019. p. 1182.
[6] PCI. PCI Bridge Design Manual. 4th Edition. Chicago, Illinois, U.SA: Precast/Prestressed Concrete Institute; 2024. p. 1954 (Customary US units). ⟨https://www.pci.org/ItemDetail?iProductCode=MNL-133-23&Category=TRANSPORT⟩.
[7] Whelchel RT, Williams CS, Frosch RJ. Live-Load Distribution of an Adjacent Box-Beam Bridge: Influence of Bridge Deck. PCI J 2021;66(6):51–71. https://doi.org/10.15554/pcij66.6-03.
[8] Zokaie T. AASHTO-LRFD Live Load Distribution Specifications. Journal of Bridge Engineering, VA, U.S.A.: American Society of Civil Engineers, Reston; 2000. 5(2): 131–138. https://doi.org/10.1061/(ASCE)1084-0702(2000)5:2(131).
[9] BridgeTech Inc. Simplified Live Load Distribution Factor Equations. NCHRP Report 592. Washington, DC, U.S.A.: National Cooperative Highway Research Program, Transportation Research Board, National Research Council; 2007. p. 137. ⟨https://www.trb.org/publications/nchrp/nchrp_rpt_592.pdf⟩. NCHRP Report 592.
[10] Cross B, Vaughn B, Panahshahi N, Petermeier D, Siow YS, Domagalski T. Analytical and Experimental Investigation of Bridge Girder Shear Distribution Factors. J Bridge Eng 2009;14(3):154–63.
[11] Just DJ, Walley WJ. Torsion of solid and hollow rectangular beams. J Struct Div 1979;105(9). https://doi.org/10.1061/JSDEAG.0005230.
[12] Nouri G, Ahmadi Z. Influence of skew angle on continuous composite girder bridge. J Bridge Eng 2012;17(4):617–23. https://doi.org/10.1061/(ASCE)BE.1943-5592.0000273.
[13] Ebeido T, Kennedy JB. Shear distribution in simply supported skew composite bridges. Can J Civ Eng 1995;22(6):1143–54. https://doi.org/10.1139/l95-132.
[14] Ebeido T, Kennedy JB. Girder moments in simply supported skew composite bridges. Can J Civ Eng 1996;23(4):904–16. https://doi.org/10.1139/l96-897.
[15] Theoret P, Massicotte B, Conciatori D. Analysis and Design of Straight and Skewed Slab Bridges. J Bridge Eng 2011;17(2):289–301. https://doi.org/10.1061/(ASCE)BE.1943-5592.0000249>.
[16] Maharjan Y, Dhungel S, Guner S. Innovative Evaluation of Precast, Prestressed Adjacent Box Beam Bridges. Columbus, OH, USA: Final project report, Department of Civil and Environmental Engineering, The University of Toledo, OH, USA, prepared for the Ohio Department of Transportation; 2025. ⟨https://www.utoledo.edu/engineering/faculty/serhan-guner/docs/R5-ODOT-ADBOX-2025.pdf⟩.
[17] American Concrete Institute. Building Code for Structural Concrete (ACI 318-25) and Commentary. MI, U.S.A.: American Concrete Institute, Farmington Hills; 2025. p. 702.
[18] Vecchio FJ, Collins MP. The modified compression-field theory for reinforced concrete elements subjected to shear. ACI J 1986;83(2):219–31. http://vectoranalysisgroup.com/journal_publications/jp2.pdf.
[19] Holt J, Bayrak O, Okumus P, Stavridis A, Murphy T, Panchal D, Dutta A, Randiwe A. Concrete Bridge Shear Load Rating Guide and Examples: Using the Modified Compression Field Theory. Report No. FHWA-HIF-22-025. Washington, DC, U.S.A.: Federal Highway Administration; 2022. p. 164. ⟨https://rosap.ntl.bts.gov/view/dot/62795⟩.
[20] Grubb MA, Wilson KE, White CD, Nickas WN. Load and Resistance Factor Design (LRFD) for Highway Bridge Superstructures: Reference Manual. Washington, DC, U.S.A.: Federal Highway Administration; 2015. p. 1698. ⟨https://rosap.ntl.bts.gov/view/dot/43721⟩.
[21] Maharjan Y, Guner S. Ad-Box©: Adjacent Box Beam Bridge Analysis and Rating," Excel Spreadsheet, Department of Civil and Environmental Engineering. OH, USA: The University of Toledo; 2025. ⟨https://www.utoledo.edu/engineering/faculty/serhan-guner/ADBOX.html⟩. <https://www.utoledo.edu/engineering/faculty/serhan-guner/docs/AD-BOX-V2.6.xlsm>.
[22] ODOT. Design Standard PSBD-02-07: Prestressed Concrete Box Beam Details. Revised 2011. Columbus, Ohio, U.SA: Ohio Department of Transportation; 2007–18. p. 4. ⟨https://www.dot.state.oh.us/SCDs/Structural/PSBD-2-07.pdf⟩.
[23] ODOT. ODOT Bridge Design Manual. 2020 Edition. Columbus, Ohio, U.SA: Ohio Department of Transportation; 2020. p. 536.. ⟨https://www.transportation.ohio.gov/working/engineering/structural/bdm⟩ (Customary US units).
[24] AASHTOWare. Bridge Rating (BrR). Version 7.5.1 [Software]. Washington, DC, U.S.A: American Association of State Highway and Transportation Officials; 2024.